Original Article

Eur J Breast Health 2018; 14: 39-45
DOI: 10.5152/ejbh.2017.3543

MR Imaging Features of Tubular Carcinoma: Preliminary Experience in Twelve Masses

Ravza Yılmaz[1], Zuhal Bayramoğlu[1], Selman Emirikçi[2], Semen Önder[3], Artur Salmaslıoğlu[1], Memduh Dursun[1], Gülden Acunaş[1], Vahit Özmen[2]

[1]Department of Radiology, İstanbul University School of Medicine, İstanbul,Turkey
[2]Department of General Surgery, İstanbul University School of Medicine, İstanbul,Turkey
[3]Department of Pathology, İstanbul University School of Medicine, İstanbul,Turkey

ABSTRACT

Objective: We retrospectively analyzed the magnetic resonance (MR) imaging features and diffusion-weighted imaging findings of the 12 masses of 10 patients with tubular carcinoma (TC), including mammography and sonography findings.

Materials and Methods: Mammographic, sonographic and magnetic resonance imaging features in 12 histopathologically confirmed masses diagnosed as TC of the breast within 10 patients were evaluated. Morphologic characteristics, enhancement features, apparent diffusion coefficient (ADC) values were reviewed.

Results: On mammography (n=5), TC appeared as high density masses with indistinct, spiculated or obscured margins. Sonographically, TC appeared as a hypoechoic appearance (n=12) with posterior acoustic shadowing in nine. On MR imaging, the margins of ten of twelve masses were irregular. Internal enhancement patterns were heterogeneous in 10 patients. Dynamic enhancement patterns illustrated plateau kinetics (n=8). On the T2-weighted images 4 masses were hypointense, and 8 were hyperintense; hypointense internal septation was found in seven of these. Tubular carcinoma appeared as hyperintense on diffusion-weighted imaging with ADC values of 0.85±0.16x10-3 mm^2/s that was lower than the normal parenchyma of 1.25±0.25x10-3 mm^2/s.

Conclusion: According to our study with a limited number of cases, tubular carcinomas can be described as hyperintense breast carcinomas with or without dark internal septation like appearance on T2-weighted images. Low ADC values from DW imaging can be used to differentiate TC from hyperintense benign breast lesions.

Keywords: Tubular cancer, ultrasonography, magnetic resonance imaging, diffusion weighted imaging, hyperintense breast cancer

Cite this article as: Yılmaz R, Bayramoğlu Z, Emirikçi S, Önder S, Salmaslıoğlu A, Dursun M, Acunaş G, Özmen V. MR Imaging Features of Tubular Carcinoma: Preliminary Experience in Twelve Masses. Eur J Breast Health 2018; 14: 39-45

Introduction

Tubular carcinoma (TC), a rare histologic type of invasive malignancy, forms almost 1% to 5% of the breast carcinomas (1-3). Histologically, TCs are composed of ductal epithelial tubules that spontaneously burst into the stroma and are covered by a single ductal epithelium cell and are directly associated with myoepithelial cells adjacent to the stroma (4). The absence of myoepithelial cells was detected with p53 immunostaining in tubular carcinomas. It has a more convenient prognosis than less well-differentiated invasive breast carcinomas, with fewer metastases to axillary lymph nodes and better survival .rates (5-7). Despite these tumors may be discovered as large palpable masses, they are usually detected when they are less than 1 cm in diameter (8). Ultrasonography (US) or mammography (MG) features of TC have been described a few times (9-12), however, little has been published about its magnetic resonance (MR) imaging appearance (13, 14). The most frequent mammographic finding of tubular carcinoma has been described as an irregular shaped mass with spiculated margins. On sonography, tubular carcinomas are usually seen as hypoechoic masses with ill-defined margins and posterior acoustic shadowing. Ghai et al. (14) reported MR imaging findings of pure TCs but their series included only three cases with nonspecific findings. Linda et al. (13) reported that TC had low-intermediate signal on T2-weighted images and heterogeneous enhancement with Type 2 curve (persistent enhancement) on dynamic analysis, but without mentioning the number of patients or a study. The purpose of this work was

Address for Correspondence :
Ravza Yılmaz, e-mail: ravzaylmz@gmail.com

Received: 18.04.2017
Accepted: 26.06.2017

to assess the MR imaging features of TC of the breast. This study is the first MR imaging study of tubular carcinoma in the available literature.

Materials and Methods

A retrospective evaluation for 4050 breast carcinomas diagnosed at a single institution between February 2001 and February 2016, revealed 39 histopathologically proven masses of pure TC of the breast. Imaging findings were retrospectively analyzed. Twenty-one of TC were identified in mammographic screening with the addition of ultrasonography. In 18 cases, patients had clinical complaints so the masses were detected during diagnostic evaluation with MG and US. Ten of the 39 patients who underwent MR imaging in our institution were included in our study. This study was approved by local ethics committee.

All study examinations were performed on a 1.5T system (Achieva, Philips Medical Systems, Best, The Netherlands) by using a dedicated four-channel breast coil. T2-weighted (T2-W) fat-saturated turbo spin echo (TR/TE: 4130/120ms; matrix, 270x234; FOV, 340x400mm; slice thickness, 2mm; NEX, 3) and T1-weighted (T1-W) turbo spin echo (TR/TE: 498/10ms; matrix, 270x265; FOV, 340x400mm; slice thickness; 2mm NEX, 2) were performed in axial planes. For this purpose a 2D spin-echo echo-planar imaging (EPI) sequence (TR, 15180 ms, fractional TE, 86 ms; FOV, 340x340 mm; matrix, 228x226; slice thickness, 3 mm; NEX, 2 mm) was used. Sensitizing diffusion gradients in three orthogonal directions with b values of 50, 400, and 800 s/mm2 were obtained. Dynamic fat-saturated 3D T1-W turbo field echo sequence (THRIVE) (TR/TE, 7/4.6ms; matrix, 340x342; NEX, 2; FOV, 336x340mm) images in the axial plane were taken once before and seven times following the administration contrast agent. Contrast materials based on gadolinium at a dose of 0.2 mmol/kg of body weight was administered with a power injector followed saline flush. Subtracted images were evaluated and the time-signal intensity curves of the masses were drawn and interpreted. The turbo field echo in sagittal plan (TR/TE, 8.2/4.7ms; matrix, 246x252; NEX, 3; FOV, 200x210 mm) was obtained after the administration of contrast in the 3D array.

The MR imaging, US and MG findings were characterized by consensus reading according to the American College of Radiology's Breast Imaging Reporting and Data System (BI-RADS) Atlas 5th edition (15). Two radiologists with six and four years of experience in breast imaging interpreted the MR images of TCs by processing in Extended MR workstation. Lesions were categorized as follows: focus, mass and non-mass enhancement. Masses were interpreted as margin (smooth, spiculated or irregular), shape (oval, irregular, round), and internal enhancement pattern (rim enhancement, non-enhancing internal septation, heterogeneous, homogeneous). Non-mass enhancement was evaluated as the internal enhancement pattern (homogeneous, heterogeneous, clumped, clustered ring) and distribution (focal, linear, regional, segmental or diffuse). The time-signal intensity curves (progressive, plateau, washout) with early (initial) enhancement findings (fast, medium, slow) of lesions were obtained. Apparent diffusion coefficient (ADC) maps were generated on the Extended MR WorkSpace 2.6.3.5 workstation. ADC values were calculated using whole-measurement method. A freehand region of interest was drawn above the enhancing component of the mass throughout the entire dynamic series and included not more than 3-4 pixels. Regions of interest were drawn on the b = 800 s/mm2 images round the mass, with reference to the information from T2-W and subtraction sequences of breast MR study. ADC value of the TC and contralateral normal parenchyma of the breast were measured three times. Measurement of ADC of normal breast parenchyma was compared with ADC of TC.

US and MG findings of ten patients were analyzed. The mammographic findings were analyzed for asymmetry and masses. Masses were analyzed for density (high, equal and low), shape (irregular, oval, round) and margins (circumscribed, spiculated, obscured, indistinct and microlobulated). Accompanying architectural distortions and calcifications were also analyzed. Ultrasonography was used to evaluate lesion shape, margin characteristics, echogenicity and posterior acoustic features.

Patients underwent breast-conserving surgery (n=7) or mastectomy (n=3) with sentinel lymph node sampling. Preoperatively, the nonpalpable lesions were localized sonographically in seven patients. Three patients underwent mastectomy because of patient preference, the presence of invasive ductal carcinoma and the presence of ductal carcinoma in situ in the different quadrant of the same breast.

Table 1. Sonographic and mammographic features of tubular carcinoma

Mass	US-Echogenicity	US-Shape, Border	US-Attenuation	MG Findings
1	hypoechoic	irregular, indistinct	acoustic shadowing	high-density irregular mass with indistinct margin
2	hypoechoic	irregular, indistinct	acoustic shadowing	asymmetric density
3	hypoechoic	irregular, microlobulated	acoustic shadowing	high-density irregular mass with obscured margin
4	hypoechoic	irregular, angular	normal sound transmission	high-density irregular mass with indistinct margin
5	hypoechoic	irregular, microlobulated	acoustic shadowing	asymmetric density
6	hypoechoic	irregular, microlobulated	acoustic shadowing	dense parenchyma
7	hypoechoic	irregular, spiculated	acoustic shadowing	dense parenchyma
8	hypoechoic	irregular, indistinct	acoustic shadowing	dense parenchyma
9	hypoechoic	irregular, spiculated	acoustic shadowing	high-density irregular mass with spiculated margin
10	hypoechoic	irregular, angular	normal sound transmission	not visible
11	hypoechoic	irregular, angular	normal sound transmission	not visible
12	hypoechoic	irregular, microlobulated	shadowing	high-density oval mass with indistinct margin

US: ultrasonography; MG: mammography

Table 2. MR imaging features of tubular carcinoma

masses	Age		Right/ left	Size-MR (mm)	Size-Pathology (mm)	T2-weighted	T1-weighted	Shape	pattern	Enhancement Margin	Initial phase	Delayed phase	ADC-m, ADC-p	ln-p	satellite	adc-m	adc-p
1	47	upper-outer	right	8	9	hyperintense septation	hypointense	irregular	heterogeneous	spiculated	fast	persistent	0.9–1.3	0	0	0,9	1,3
2	48	upper-inner	left	7	6	hypointense	hypointense	irregular	heterogeneous	irregular	medium	persistent	0.8–1.2	0	0	8	1,2
3	49	upper-outer	right	16	15	hyperintense	hypointense	irregular	heterogeneous	irregular	fast	plateau	0.9–1.1	1, micrometastasis	0	0,9	1,1
4	45	upper-inner	left	8	8	hyperintense septation	hypointense	irregular	homogeneous	irregular	fast	washout	0.8–1.4	0	0	0,8	1,4
5	58	upper-outer	right	9	7	hypointense	hypointense	irregular	heterogeneous	irregular	fast	plateau	0.6–1	0	1	0,6	1
6	58	upper-outer	right	10	10	hypointense	hypointense	irregular	heterogeneous	irregular	fast	plateau	0.6–1	0	1	0,6	1
7	48	lower-outer	right	9	10	hyperintense	hypointense septation	irregular	homogeneous	irregular	fast	plateau	1.1–1.8	0	0	1,1	1,8
8	48	upper-outer	left	7	6	hyperintense septation	hypointense	irregular	heterogeneous	irregular	fast	plateau	1.1–1.5	0	0	1	1,5
9	42	upper-inner	left	15	25	hyperintense septation	hypointense	oval	heterogeneous	spiculated	fast	plateau	0.8–1	0		0,8	1
10	42	upper-inner	left	10	11	hyperintense septation	hypointense	irregular	heterogeneous	irregular	fast	plateau	0.7–1	0	0	0,7	1
11	37	upper-outer	right	5	5	hyperintense septation	hypointense	oval	heterogeneous	irregular	medium	plateau	1–1.4	0	0	1,1	1,4
12	48	lower-outer	left	5	4	hypointense	hypointense	oval	heterogeneous	irregular	fast	persistent	1–1.4	0	0	0,9	1,4

MR: magnetic resonance; ADC: apparent diffusion coefficient; Size-MR: size-magnetic resonance; Size-P: Lesion size-histopathology

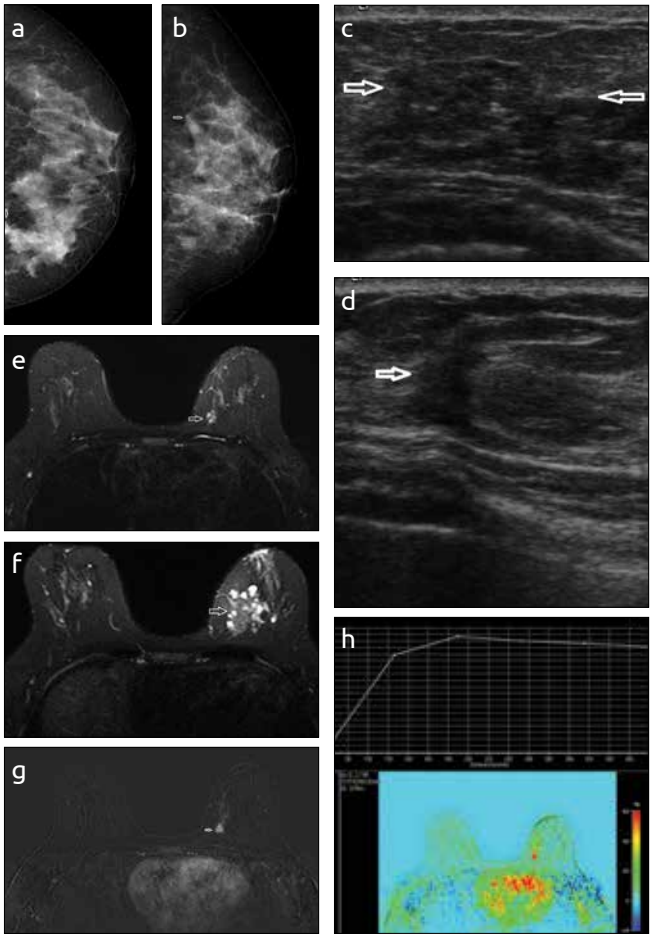

Figure 1. a-h (mass 4). A 45-years-old woman with palpable mass in the lower-inner quadrant of the left breast. Craniocaudal (a) and mediolateral (b) oblique mammography images showed not only a 30x15 mm high-density irregular mass with amorphous calcification in the lower-inner quadrant, but also 8x7mm high-density irregular mass with indistinct margins (arrow), which proved to be tubular carcinoma in the upper-inner quadrant of heterogeneous dense parenchyma. Sonography (c) of that palpable area showed a predominantly solid mass with internal cystic spaces and calcification (arrows). Tubular carcinoma was an irregular hypoechoic mass (d) with angulated border (arrow). Axial T2-weighted images with fat suppression shows 8 mm hyperintense lobulated tubular carcinoma with dark internal septation (arrow) (e) and hypointense mass with milimetric cysts that proved to be stromal fibrosis (f). TC shows homogenous contrast enhancement with Type-3 dynamic analysis on T1-weighted gadolinium-enhanced subtraction image (2.second) (g), (h)

Statistical Package for Social Sciences (SPSS) software version 17 (SPSS Inc, Chicago, IL, US) was used for statistical analyses. Data are presented as follows: mean±standard deviation or median with range, as appropriate. The frequencies of involvement in each quadrant, additional lesion, the presence of suspicious lymph nodes and magnetic resonance imaging findings were also analyzed. The Mann-Whitney U test was used for comparing the continuous variables of two samples. $p<0.05$ was considered as a sign of a significant difference. Each eligible woman was informed and signed the consent form.

Results

Ten patients with twelve masses of TC were evaluated. Our patients were aged between 37 and 58 years (mean age, 47) at the time of the diagnosis. There was no positive risk factor for breast cancer in any patient. Three patients were considered to be diagnostic for firm-palpable mass on physical examination. In seven patients, TC was diagnosed on screening mammography and additionally on ultrasonography; the other cases were symptomatic and were evaluated diagnostically. MG was negative in 5 (42%) patients. US and MR imaging was positive in all patients (TC could be seen with second look US in two patients). Six of the twelve masses were in the left breast (50%). The quadrant frequency in the twelve breasts was upper-outer (50%), upper-inner (33%), and lower-outer (17%).

Mammography showed TC as a high-density mass in 5 (42%) patients and as asymmetry in 2 (16%) patients. No architectural distortion or suspicious calcification was seen in any patients on MG. Masses were irregular shaped with microlobulated margin in 1 patient, indistinct margin in 2 patients and spiculated margin in 1 patient. An oval shaped mass with indistinct margin was seen in only one patient. US was positive in all patients of 12 masses (1 multifocal and 1 bilateral). All masses were hypoechoic (n=12) with nine of them with posterior acoustic shadowing. All patients had masses with irregular shapes. The margins of the masses were microlobulated in 4 (33%) patients, angular in 3 (25%) patients, indistinct in 3 (25%) patients, and spiculated in 2 (17%) patients. US and MG imaging findings are presented in Table 1.

The amount of fibroglandular tissue in patients with TC on MRI was almost entirely fat in 1/12, scattered fibroglandular tissue in 2/12, heterogeneous fibroglandular tissue in 4/12, and extreme fibroglandular tissue in 5/12 of patients. All TCs were visible as masses with a total of twelve (1 bilateral and 1 multifocal) on MR imaging. The size of the masses on MR imaging varied from 5 to 16 mm (mean, 9 mm). The masses were irregular (n=9) and oval shaped (n=3). The margins of the masses were irregular in 10 patients, and spiculated in 2 patients on MR imaging. The patterns of internal enhancement were found to be homogeneous in 2 patients and heterogeneous in 10 patients. The time-signal intensity curve (delayed enhancement phase) showed progressive enhancement (Type-1) in 3 (25%) masses, a plateau enhancement (Type-2) in 8 (67%) masses, and a washout enhancement (Type-3) in 1 (8%) mass. Initial enhancement phase was fast in ten masses and medium in two masses. All TCs showed a hypointense signal on T1-W images. Mass signals were variable on T2-W, hypointense in 4 masses, and hyperintense in 8 masses. The hypointense internal septation-like appearance was observed in seven of the hyperintense masses on T2-W images (Figure1). The mean ADC value of tubular carcinoma was calculated ($0.85\pm0.16\times10^{-3}$ mm^2**/s**) as lower than the mean ADC value of normal parenchyma ($1.25\pm0.25\times10^{-3}$ mm^2**/s**) (Figure 2). The difference between TC and normal parenchyma ADC values was significant ($p<0.05$). MR imaging findings are provided in Table 2. MR imaging did not provide additional contribution to MG and US in our study (multifocality, suspicious lymph node (LN) or different findings).

Histopathological examination of the tumor size ranged from 4 to 25 mm (mean, 9.6 mm). A total of 12 masses were seen in the 10 patients. One patient had bilateral tubular carcinoma (Figure 3). The tumor was multifocal in one patient, who also showed DCIS in another quadrant of the same breast. Axillary lymph node metastasis was present in only one patient as micrometastases; the tumor size was 15mm in that patient (Figure 4).

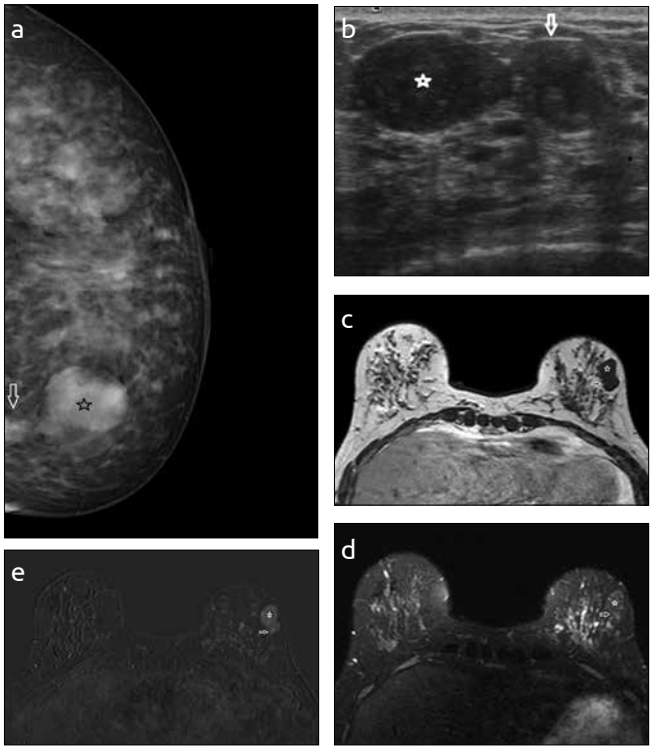

Figure 2. a-e (mass 12). A 48-years-old woman with tubular carcinoma. Craniocaudal mammography (a) shows high-density oval mass with indistinct margins (arrow) adjacent to fibroadenoma (asterisk) on outer quadrant of left breast. Tubular cancer cannot be seen on mediolateral oblique projection. Sonographically, irregular shaped, heterogeneous, microlobulated tubular carcinoma with posterior shadowing (arrow) and oval shaped hypoechoic fibroadenoma with well-defined margins (asterisk) were detected (b). Also a thin fat plane was seen between masses. Axial T1-weighted without fat suppression (c) and T2-weighted with fat suppression (d) images show 5mm hypointense tubular carcinoma (arrow) and fibroadenoma (asterisk). TC (arrow) shows heterogeneous contrast enhancement on T1-weighted gadolinium-enhanced subtraction image (2.second) (e)

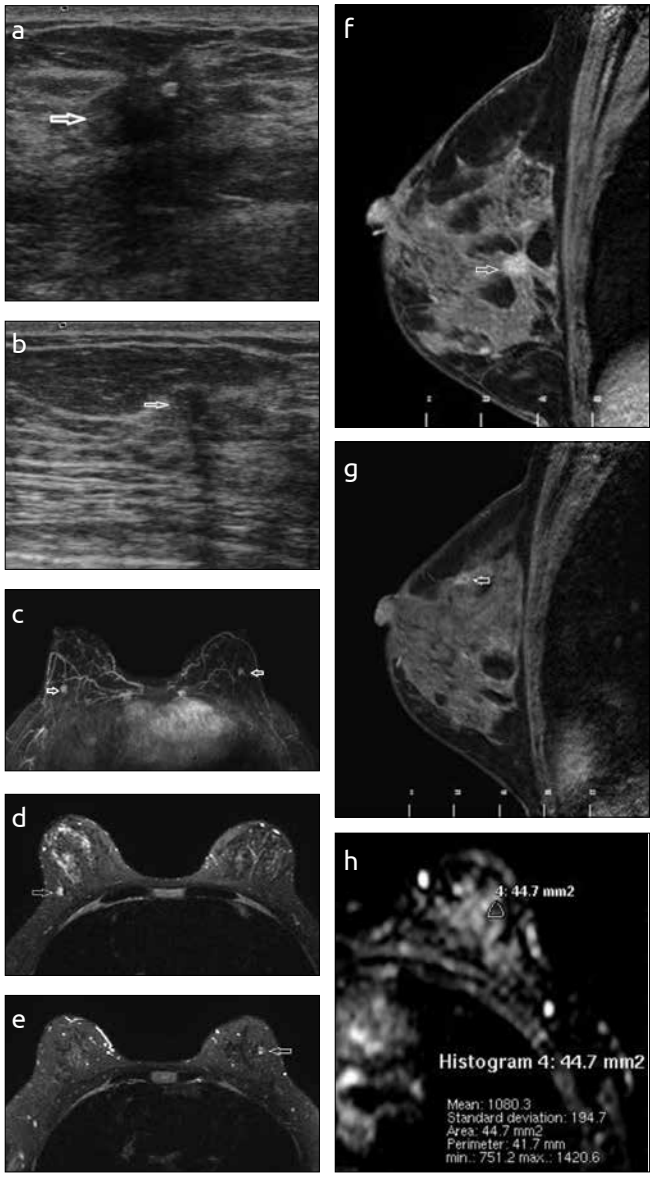

Figure 3. a-i (mass 7 and mass 8). A 48-years-old woman with bilateral tubular carcinoma that was negative on MG. Sonography detected an irregular shaped mass with spiculated margins on the right breast (a) and irregular shaped mass with indistinct margins on the left breast (b). Axial maximum intensity projection of a contrast enhanced T1-weighted three-dimensional spoiled gradient-echo image (c) shows bilateral tubular carcinomas (arrows). Axial T2-weighted with fat suppression images show 9mm hyperintense mass with slightly visible internal septation on the right breast (arrow) (d) and 7 mm hyperintense mass with prominent hypointense internal septation on the left breast (e). In the sagittal plane of post-contrast fat suppression images, mass on the right breast enhanced homogenously (arrow) (f) and mass on the left breast enhanced heterogeneously (arrow) (g). Apparent diffusion coefficient (ADC) map reveals 1.12×10^{-3} mm^2/s within mass on the right breast (h) and 1.08×10^{-3} mm^2/s on the left breast (i)

Discussion and Conclusion

A few articles have been reported regarding the MR findings of TC (13, 14). Because tubular carcinoma was only partially mentioned in these articles, little information was provided and MR imaging features for this type of tumor were nonspecific. MR imaging is performed very rarely in patients who are diagnosed with TC because of typical malignant features on MG and US and due to small size. In our series, all of the TC appeared as mostly irregular shaped masses with indistinct margin classified according to the BI-RADS 5th edition (15). Tubular carcinoma sizes were too small in general to evaluate margins accurately on MR imaging compared to MG and US. So, spiculated margins, which constitute a common finding for this type of cancer, were not observed frequently on MR imaging. TC showed hypointense signal on T1-W images in all masses just like other breast carcinomas, but in seven of the masses there was hyperintense signal with dark internal septations on T2-W images in our study. Breast carcinoma with high signal intensity on T2-W was reported many times in the literature, but there is no information about TC (16, 17). In our series, high signal intensity on T2-W images was considered to be a MR feature of tubular carcinoma. Meanwhile hypointense internal septation-like appearance was seen in most of the hyperintense tubular carcinomas, which was a different finding from most of the other cancers. The pattern of internal enhancement was heterogeneous in most of the tubular carcinomas. Consistent with other breast cancers, our results showed that the kinetic curve obtained from contrast enhanced MR imaging of TC exhibits a fast initial contrast enhancement pattern, followed by a plateau pattern. Linda et al. (13) reported spiculated shape, ill-defined margin, low-intermediate signal on T2-W and heterogeneous

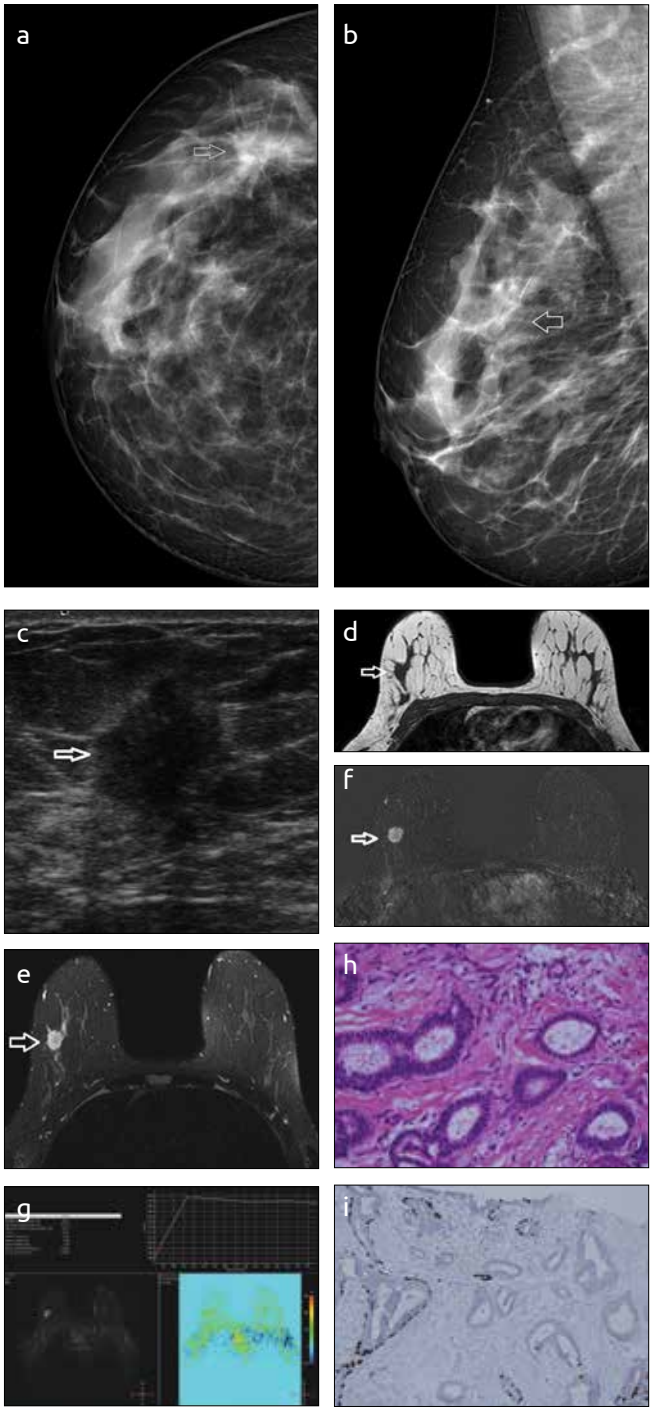

Figure 4. a-i (mass 3). A 49-years-old woman with tubular carcinoma who had axillary lymph node metastasis. Craniocaudal (a) mammography shows high-density mass with obscured margins in the outer quadrant of the right breast (arrow), but the mass was unclear on mediolateral oblique (b) MG. Ultrasonography (c) image reveals irregularly shaped tubular carcinoma with microlobulated margins (arrow), also posterior shadowing is seen. Axial T1-weighted image without fat suppression (d) shows a 16 mm irregularly shaped hypointense tubular carcinoma (arrow). Mass (arrow) is heterogeneous hyperintense on T2-weighted fat suppression image (e). TC shows heterogeneous contrast enhancement (arrow) (f) with Type-2 dynamic analysis on T1-weighted gadolinium-enhanced subtraction image (2. second) (g). Infiltrating tubules with angular shape in a desmoplastic stroma (H.E, x20, original magnification) (h). No myoepithelial cells were detected with p63 immunostaining in tubular carcinoma (p63, x10, original magnification) (i)

enhancement with persistent kinetic curve in their article about MR features of tubular carcinoma. Ghai et al. (14) reported three tubular carcinomas that did not enhance on MR imaging. These were the only findings reported in the imaging literature about TC characteristics on MR imaging. We had difficulty in defining morphologic, kinetic and diffusion characteristics of lesions smaller than 7 mm. US findings were useful for characterization of subcentimeter lesions on MR imaging. In one patient, we decided to designate a 5 mm lesion as a mass because of its space occupying nature on axial and sagittal images, hypointense signal on T2-W images and its visibility on US.

Diffusion-weighted MR imaging demonstrates high accuracy in differentiating malignancy from benignancy by measuring the ADC in breast lesions (18, 19). We measured the mean ADC values of TC and ADC of normal contralateral parenchyma and compared each other. According to our results, the mean ADCs of the TC ($0.85\pm0.16x10^{-3}$ mm^2**/s**) were lower than breast parenchyma ($1.25\pm0.25x10^{-3}$ mm^2**/s**). Previous studies have shown that ADC values of malignant lesions are significantly lower than benign lesions and parenchymal values (18, 20-22). However, there are no reports about ADC values to differentiate breast carcinomas from one other. Our results on calculated ADC values demonstrated that TC had similar ADC values with previously studied invasive breast carcinomas (18-22). Even though hyperintense signal with dark internal septations of TC on T2-W images of MR imaging is similar to fibroadenoma, dynamic analysis with early and delayed enhancement patterns, ADC values and advanced age help to differentiate TC from this benign entity on MR imaging.

Tubular carcinoma has been reported to be related with other types of carcinomas and associated with other histologic entities (4, 23, 24). In this study, one patient with DCIS in another quadrant of the same breast and one patient with invasive ductal carcinoma in the same quadrant were reported. TC has been reported to have a low recurrence rate (25). No deaths as a result of distant metastasis or cancer were seen in our study. Axillary LN metastases are rare in patients with TC. Only one patient had LN micrometastasis, and that patient had a higher mean tumor size (15 mm) in our study.

The mammography and sonography characteristics of this rare tumor have been discussed in several reports (5, 9, 10, 11, 23). The described features on MG and US were not specific for TC with suspicion of malignancy. Common finding of the breast tubular carcinoma is the irregular shaped mass with spiculated margin on both US and MG (9, 11, 23). In our series, on mammography, tubular carcinomas were usually high-density, irregular shaped masses with indistinct or spiculated margins. Almost all tubular carcinomas in the literature are hypoechoic masses with posterior acoustic shadowing (9, 11). In our study all tubular carcinomas were irregular shaped with hypoechoic echotexture. Most of them (73%) had posterior acoustic shadowing on US.

Several limitations of this study should be acknowledged. This study was retrospective in design and a case collection study. There is no a case control study, therefore it remains unclear whether or not these MR characteristics are specific findings. New studies with larger populations and a comparative-prospective nature are required for further evaluation of MR imaging features in TC, maybe to differentiate them from other breast carcinomas and fibroadenomas.

In conclusion, the present study was the first to report two important MR imaging features of pure tubular carcinomas. Tubular carcinomas may exhibit high signal intensity and dark internal septation-like ap-

pearance on T2-W images. In such cases low ADC values from DW imaging may useful differentiating TC from hyperintense benign breast lesions.

Ethics Committee Approval: Ethics committee approval was received for this study from the ethics committee of İstanbul Universty Faculty of Medicine.

Informed Consent: Written informed consent was obtained from patient who participated in this study.

Peer-review: Externally peer-reviewed.

Author Contributions: Concept - R.Y., Z.B.; Design - R.Y, A.S.; Supervision - R.Y., M.D.; Resources - S.E., S.O.; Materials - R.Y., S.O.; Data Collection and/or Processing - R.Y., S.E.; Analysis and/or Interpretation - R.Y., V.Ö.; Literature Search - R.Y., Z.B.; Writing Manuscript - R.Y., A.S.; Critical Review - V.Ö., G.A.

Acknowledgements: Authors would like to thank patients who participated this study.

Conflict of Interest: No conflict of interest was declared by the authors.

Financial Disclosure: The authors declared that this study has received no financial support**.**

References

1. Sullivan T, Raad RA, Goldberg S, Assaad SI, Gadd M, Smith BL, Powell SN, Taghian AG. Tubular carcinoma of the breast: a retrospective analysis and review of the literature. Breast Cancer Res Treat 2005; 93: 199-205. (PMID: 16142444) [CrossRef]
2. Cabral AH, Recine M, Paramo JC, McPhee MM, Poppiti R, Mesko TW. Tubular carcinoma of the breast: an institutional experience and review of the literature. Breast J 2003; 9: 298-301. (PMID: 12846864) [CrossRef]
3. Rakha EA, Lee AH, Evans AJ, Menon S, Assad NY, Hodi Z, Macmillan D, Blamey RW, Ellis IO. Tubular carcinoma of the breast: further evidence to support its excellent prognosis. J Clin Oncol 2010; 28: 99-104. (PMID: 19917872) [CrossRef]
4. Page DL, Anderson TJ. Infiltrating carcinomas: major histological types. Diagnostic histopathology of the breast. 1987. p. 193–235.
5. Peters GN, Wolff M, Haagensen CD. Tubular carcinoma of the breast: clinical pathologic correlations based on 100 cases. Ann Surg 1981; 193: 138-149. (PMID: 7469549) [CrossRef]
6. Leibman AJ, Lewis M, Kruse B. Tubular carcinoma of the breast: mammographic appearance. AJR Am J Roentgenol 1993; 160: 263-265. (PMID: 8424330) [CrossRef]
7. Does PH, Norris HJ. Well-differentiated (tubular) carcinoma of the breast: a clinicopathologic study of 145 pure and mixed cases. Am J Clin Pathol 1982; 78: 1-7. (PMID: 6285690) [CrossRef]
8. Rosen PP. Tubular carcinoma. In: Rosen PP, editor. Rosen's breast pathology. Philadelphia: Lipincott-Raven; 1997. p. 321–334.
9. Günhan-Bilgen I, Oktay A. Tubular carcinoma of the breast: mammographic, sonographic, clinical and pathologic findings. Clin Imaging 2007; 31: 295-296. [CrossRef]
10. Elson BC, Helvie MA, Frank TS, Wilson TE, Adler DD. Tubular carcinoma of the breast: mode of presentation, mammographic appearance, and frequency of nodal metastases. AJR Am J Roentgenol 1993; 161: 1173-1176. (PMID: 8249721) [CrossRef]
11. Vega A, Garijo E. Radial scar and tubular carcinoma: mammographic and sonographic findings. Acta Radiol 1993; 34: 43-47. (PMID: 8427748) [CrossRef]
12. Sheppard DG, Whitman GJ, Huynh PT, Sahin AA, Fornage BD, Stelling CB. Tubular carcinoma of the breast: mammographic and sonographic features. AJR Am J Roentgenol 2000; 174: 253-257. (PMID: 10628489) [CrossRef]
13. Linda A, Zuiani C, Girometti R, Londero V, Machin P, Brondani G, Bazzocchi M. Unusual malignant tumors of the breast: MRI features and pathologic correlation. Eur J Radiol 2010; 75: 178-184. (PMID: 19446418) [CrossRef]
14. Ghai S, Muradali D, Bukhanov K, Kulkarni S. Nonenhancing breast malignancies on MRI: sonographic and pathologic correlation. AJR Am J Roentgenol 2005; 185: 481-487. (PMID: 16037524) [CrossRef]
15. Sickles EA, D'Orsi C. Follow-up and outcome monitoring. In: ACR BI-RADS® atlas, breast imaging and reporting and data system. Reston, VA: American College of Radiology, 2013. Footnote (a), p. 27.
16. Yuen S, Uematsu T, Kasami M, Tanaka K, Kimura K, Sanuki J, Uchida Y, Furukawa H. Breast carcinomas with strong high-signal intensity on T2-weighted MR images: pathological characteristics and differential diagnosis. Magn Reson Imaging 2007; 25: 502-510. (PMID: 17326093) [CrossRef]
17. Santamaría G, Velasco M, Bargalló X, Caparrós X, Farrús B, Luis Fernández P. Radiologic and pathologic findings in breast tumors with high signal intensity on T2-weighted MR images. Radiographics 2010; 30: 5335-48. (PMID: 20228333) [CrossRef]
18. Woodhams R, Matsunaga K, Iwabuchi K, Kan S, Hata H, Kuranami M, Watanabe M, Hayakawa K. Diffusion-weighted imaging of malignant breast tumors: the usefulness of apparent diffusion coefficient (ADC) value and ADC map for the detection of malignant breast tumors and evaluation of cancer extension. J Comput Assist Tomogr 2005; 29: 644-649. (PMID: 16163035) [CrossRef]
19. Woodhams R, Kakita S, Hata H, Iwabuchi K, Kuranami M, Gautam S, Hatabu H, Kan S, Mountford C. Identication of residual breast carcinoma following neoadjuvant chemother- apy: diffusion-weighted imaging—comparison with contrast- enhanced MR imaging and pathologic findings. Radiology 2010; 254: 357-366. (PMID: 20093508) [CrossRef]
20. Marini C, Iacconi C, Giannelli M, Cilotti A, Moretti M, Bartolozzi C. Quantitative diffusion-weighted MR imaging in the differential diagnosis of breast lesion. Eur Radiol 2007; 17: 2646-2655. (PMID: 17356840) [CrossRef]
21. Kuroki-Suzuki S, Kuroki Y, Nasu K, Nawano S, Moriyama N, Okazaki M. Detecting breast cancer with non-contrast MR imaging: combining diffusion-weighted and STIR imaging. Magn Reson Med Sci. 2007; 6: 21e7.
22. Hatakenaka M, Sodea H, Yabuuchi H, Matsuo Y, Kamitani T, Oda Y, Tsuneyoshi M, Honda H. Apparent diffusion coefficients of breast tumors: clinical application. Magn Reson Med Sci 2008; 7: 23-29. (PMID: 18460845) [CrossRef]
23. Mitnick JS, Gianutsos R, Pollack AH, Susman M, Baskin BL, Ko WD, Pressman PI, Feiner HD, Roses DF. Tubular carcinoma of the breast: sensitivity of diagnostic tecniques and correlation with histopathology. AJR Am J Roentgenol 1999; 172: 319-323. (PMID: 9930775) [CrossRef]
24. BergerAC, Miller SM, Haris MN, Roses DF. Axillary dissection for tubular carcinoma of the breast. Breast J 1996; 2: 203-208. [CrossRef]
25. Livi L, Paiar F, Meldolesi E, Talamonti C, Simontacchi G, Detti B, Salerno S, Bianchi S, Cardona G, Biti GP. Tubular carcinoma of the breast: outcome and loco-regional recurrence in 307 patients. Eur J Surg Oncol 2005; 31: 9-12. (PMID: 15642419) [CrossRef]